August 27-31, 2023
FLORENCE - ITALY
16th International Conference on Wind Engineering
ICWE 16

Evaluation of vortex-induced vibration of a box girder bridge using forced oscillation method with LES

K. Noguchi [1], Y. Ito [2], Y. Yan [3], T. Yagi [4]

[1]Kyoto University, Kyoto, Japan, noguchi.kyohei.7z@kyoto-u.ac.jp
[2]Shimizu Corporation, Tokyo, Japan, yasuaki.ito@shimz.co.jp
[3]Kyoto University, Kyoto, Japan, yan.yuxuan.d88@kyoto-u.jp
[4]Kyoto University, Kyoto, Japan, yagi.tomomi.7a@kyoto-u.ac.jp

SUMMARY:
The evaluation of the vortex-induced vibration (VIV) amplitude of a long-span bridge is necessary for a wind-resistant design. The development of high-performance computing has enabled the use of CFD, but the evaluation of response amplitudes of VIV using the free vibration method still incurs a high computational cost. The authors calculated the VIV amplitude using amplitude-dependent flutter derivatives obtained by the forced oscillation method with LES. However, the calculated VIV amplitude was overestimated than that by the experimental spring-supported free vibration method. This study investigated the effects of the approaching flow on the VIV amplitude and verified the validity of evaluating VIV based on the forced oscillation in CFD. First, wind tunnel tests with two different conditions were conducted. Then, the VIV amplitudes obtained by the forced oscillation method with LES were compared with the experimental results. VIV was accurately evaluated by appropriately setting the numerical condition including the turbulence of approaching flow and Reynolds number, which were significant on it.

Keywords: forced oscillation method, flutter derivatives, vortex-induced vibration

1. INTRODUCTION

The use of computational fluid dynamics (CFD) in engineering has been increased by the recent development of high-performance computing. However, CFD has not been adequately introduced for the wind-resistant design of a long-span bridge because aerodynamic stability must be evaluated as well as aerostatic stability. Especially, the free vibration method, which is generally used to evaluate the amplitude of vortex-induced vibration (VIV), still incurs a high computational cost. This is because the VIV amplitude increases or decreases gradually with time because of small aerodynamic damping. Thus, an alternative method is necessary to evaluate VIV amplitude using CFD for a wind-resistant design in practice.

Noguchi et al. (2020) employed the forced oscillation method, which obtained aerodynamic forces in the periodic state in less time than the free vibration method, to calculate amplitude-dependent flutter derivatives with LES. Then, the VIV amplitude with vertical one-degree-of-freedom (1DOF) was calculated based on the aerodynamic damping obtained from the flutter derivatives. However, the VIV amplitude was overestimated than spring-supported free vibration wind tunnel tests. This was probably because of the difference in turbulence of the approaching flow and Reynolds number between the calculations and experiments (Wardlaw et al., 1983).

To investigate the effects of turbulence of the approaching flow and Reynolds number on the VIV amplitude, this study obtained response amplitudes of VIV by free vibration wind tunnel tests with two different conditions. Also, the obtained VIV amplitudes were compared with the numerical results to verify the validity of evaluating VIV based on the forced oscillation in CFD.

2. EXPERIMENTAL AND NUMERICAL METHODS

Fig. 1 shows the cross-section of the target box girder bridge, which is the same as that in the previous study (Noguchi et al., 2020). The VIV amplitude with vertical 1DOF was obtained by wind tunnel tests and CFD, respectively. The side ratio of the cross-section was $B/D = 5.5$, where B = deck width and D = deck height excluding protuberances.

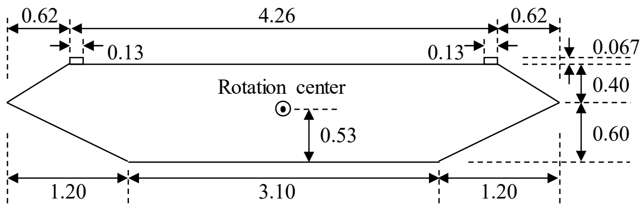

Figure 1. Cross-section (Noguchi et al., 2020).

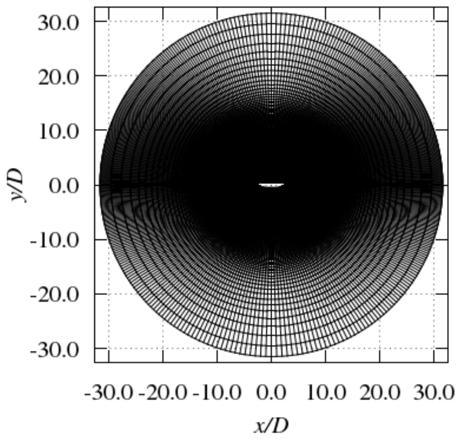

Figure 2. Computational domain (Noguchi et al., 2020).

2.1. Experimental Method

Spring-supported free vibration wind tunnel tests with two different conditions were conducted. The first one was reported by Noguchi et at. (2020). The second one was newly conducted and detailed here. The wind tunnel used was of the closed-circuit type located at Kyoto University with a working section of 1.0 m in width and 1.8 m in height. The turbulence intensity of flow at 10 m/s was <0.3%, while that in the previous study was ~1%. The height, width, and length of the section model used in the experiment were 50 mm, 275 mm, and 890 mm, respectively, which were 5/3 as large as the previous one to achieve the largest Reynolds number at the wind speed range of VIV under the limitation of the facilities (~10,000 in the present study and ~2,000 in the previous one). The model was suspended with eight coil springs in the working section under the vertical 1DOF condition. The natural frequency was 6.418 Hz, and m and δ_0 were set as m = 3.515 kg/m, δ_0 = 0.0183 at η/D = 0.10, and thus, Scruton number was $S_c = 2m\delta/(\rho B^2)$ = 1.41 (and S_c = 0.80 for Noguchi et al. (2020)), where m = equivalent mass (kg/m), δ_0 = logarithmic decrement in structural damping, η = heaving displacement, and ρ = air density.

2.2. Numerical Method

The numerical method to calculate flutter derivatives using the forced oscillation method was the same as Noguchi et al. (2020), and thus, Ito and Graham (2016; 2017), where the incompressible Navier–Stokes equation in generalized coordinates under the moving grid condition was solved. The computational domain and some other parameters also followed Noguchi et al. (2020), a summary of which is given as below. Fig. 2 shows the structured O-type grid, whose diameter was 63D. Noguchi et al. (2020) found that the spanwise domain size affected the VIV amplitude, but its impact was relatively small comparing to the other factors. Thus, the spanwise domain size was set to 1D considering the calculation cost. The vertical size of the wall-adjacent grids was D/400 and the spanwise grid size was D/20. The Reynolds number was 20,000 to utilize the simulation results of Noguchi et al. (2020). Flutter derivatives were calculated using 15 cycle oscillation after preliminary calculation of 5–15 cycle oscillation. U/fD was set to 6.0–14.0 at intervals of 1.0 except U/fD = 7.0, and η_0/D was set between 0.025 and 0.300 at intervals of 0.025. The inflow was smooth for all the simulations.

2.3. Definition of Flutter Derivatives

The unsteady lift force (L_{ae}) (downside positive) in the vertical 1DOF was defined using two flutter derivatives (H_1^* and H_4^*) as below (Scanlan and Tomko, 1971);

$$L_{ae} = {}^{1}\!/_{2}\, \rho U^2 BL \left[K H_1^* \, {}^{\dot{\eta}}\!/_{U} + K^2 H_4^* \, {}^{\eta}\!/_{B} \right] \tag{1}$$

where K = reduced frequency ($B\omega/U$), ω = circular frequency, and η = heaving displacement (downside positive). H_1^* indicates aerodynamic damping, which is defined as below:

$$H_1^* = -\frac{L_\eta \sin \Psi_L}{{}^{B}\!/_{D} \times \tilde{\omega}^2 \times {}^{\eta_0}\!/_{D}} \tag{2}$$

where L_η = nondimensional amplitude of L_{ae}, Ψ_L = phase lag between η (at the downward maximum) and L_{ae} (at the downward maximum), and $\tilde{\omega}$ = $\omega D/U$.

3. RESULTS AND DISCUSSION

Fig. 3 shows the steady-state responses of the two different free vibration wind tunnel tests (Noguchi et al., 2020). VIVs were observed from both the experiments and their wind speed ranges were almost the same. The VIV amplitude in the present study was larger than that in the previous one although the Scruton number of the present study (S_c = 1.41) was almost twice as large as that of the previous study (S_c = 0.80). Thus, the effects of the approaching flow condition and Reynolds number appeared significant on the VIV amplitude, which was probably a cause of the gaps between the wind tunnel tests and CFD in Noguchi et al. (2020).

Fig. 4 shows the flutter derivatives of H_1^* calculated by LES using the forced oscillation method for each η_0/D as a function of U/fD. H_1^* showed a clear dependence on the oscillation amplitude, especially at the wind speed range of VIV. Moreover, H_1^*, in an area of Fig. 4, was positive, which suggests the occurrence of VIV. To evaluate the VIV amplitude, the damping of the system (δ) was calculated as below, considering structural and aerodynamic damping:

$$\delta = H_1^* - 2m\delta_0/\pi\rho B^2 \tag{3}$$

δ_0 was obtained from the wind tunnel tests in the present study as a function of η/D. A positive δ describes the excitation of the vibration and a negative δ the attenuation. The steady-state response is obtained by calculating U/fD and η/D that satisfy δ = 0. As shown in Fig. 3, the

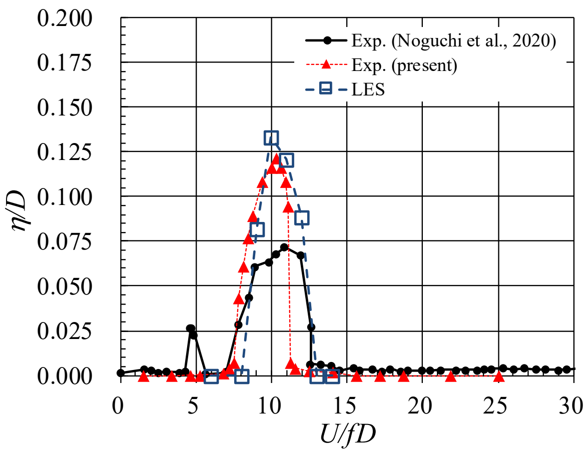

Figure 3. Velocity–amplitude diagram by the experiments and LES.

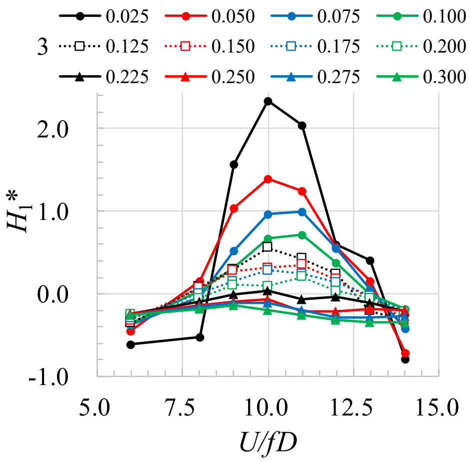

Figure 4. H_1^* as a function of U/fD and η_0/D

steady-state response of VIV obtained by the present wind tunnel tests was successfully evaluated by LES using the forced oscillation method. The wind speed ranges of VIV were almost the same, and the wind speed for the maximum amplitude by LES was comparable to that by the wind tunnel tests. The maximum amplitude obtained from the free vibration wind tunnel tests was also reproduced well by LES. Therefore, the gaps in VIV amplitude between wind tunnel tests and CFD in Noguchi et al. (2020) probably resulted from the difference in the turbulence of approaching flow and Reynolds number.

4. CONCLUSIONS

In this study, VIV was evaluated using the forced oscillation method with LES to avoid the large computational cost involved in the free vibration method. The amplitude and wind speed range of VIV were accurately calculated to reproduce those obtained from free vibration wind tunnel tests by appropriately setting the numerical condition including the approaching flow and Reynolds number, which were significant on the VIV amplitude.

ACKNOWLEDGEMENTS
The supercomputer of ACCMS, Kyoto University, was used in this study for the flow simulation.

REFERENCES

Ito, Y. and Graham, J.M.R., 2016. LES for investigation of span-wise domain size effect and evaluation of flutter de-rivatives of a box bridge. Proceedings of the 8th International Colloquium on Bluff Body Aerodynamics and Applications, Boston, Massachusetts.

Ito, Y. and Graham, J.M.R., 2017. Large eddy simulation for static and unsteady wind forces of a box girder and the effect of span-wise domain size, Journal of Japan Society of Civil Engineers (JSCE), Ser. A1 (Structural Engineering & Earthquake Engineering (SE/EE)), 73-1, 195-205. (in Japanese).

Noguchi, K., Ito, Y. and Yagi, T., 2020. Numerical evaluation of vortex-induced vibration amplitude of a box girder bridge using forced oscillation method. Journal of Wind Engineering and Industrial Aerodynamics, 196, 104029.

Scanlan, R.H. and Tomko, J.J., 1971. Airfoil and bridge deck flutter derivatives. Journal of Engineering Mechanics Division, Proc. ASCE 97-6, 1717-1737.

Wardlaw, R.L., Tanaka, H. and Utsunomiya, H., 1983. Wind tunnel experiments on the effects of turbulence on the aerodynamic behaviour of bridge road decks. Journal of Wind Engineering and Industrial Aerodynamics 14(1-3), 247-257.